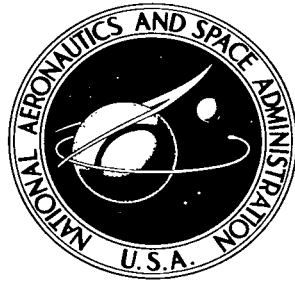


NASA TECHNICAL NOTE



NASA TN D-3789

NASA TN D-3789

1.1

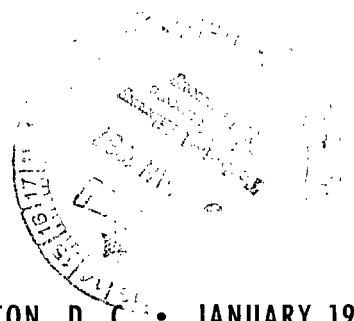


LOAN COPY: RETURN
AFWL (WLIL-2)
KIRTLAND AFB, N ME.

EXPERIMENTAL INVESTIGATION OF LIQUID-PROPELLANT REORIENTATION

by Jack A. Salzman and William J. Masica

*Lewis Research Center
Cleveland, Ohio*





EXPERIMENTAL INVESTIGATION OF LIQUID-
PROPELLANT REORIENTATION

By Jack A. Salzman and William J. Masica

Lewis Research Center
Cleveland, Ohio

NATIONAL AERONAUTICS AND SPACE ADMINISTRATION

For sale by the Clearinghouse for Federal Scientific and Technical Information
Springfield, Virginia 22151 - Price \$1.00

EXPERIMENTAL INVESTIGATION OF LIQUID-PROPELLANT REORIENTATION

by Jack A. Salzman and William J. Masica

Lewis Research Center

SUMMARY

As a part of a general study of the behavior of liquid propellants stored in space-vehicle tanks while exposed to weightlessness, the mechanism of liquid reorientation from an initially highly curved interface by low-level accelerations was examined. The study was conducted by using several propellant tank models with radii ranging from 1.27 to 5.16 centimeters and liquids possessing near 0° contact angles on the tank materials and having viscosities of the order of unity. The results of this study indicate that, while liquid rebounding or geysering will occur in most practical reorientation maneuvers, there exists a distinct region in which geysering will not occur. A criterion consisting essentially of a dimensionless Weber number grouping successfully delineated the regions of geysering and no geysering within experimental limitations. Quantitative results of liquid accumulation rates that would allow time estimates for complete liquid reorientation are heavily dependent on overall geyser dynamics.

INTRODUCTION

The major objectives of liquid-propellant management during coasting flight, where environments with very low Bond numbers (ratio of acceleration to capillary forces) are frequently encountered, are efficient engine restart capabilities and, in the case of cryogenics, an efficient venting mode to maintain tank pressurization control. The use of small auxiliary thrusters has been proposed to maintain proper propellant orientation by inducing a low body force in the direction of main-engine thrust. The success of the auxiliary thrust method depends on the ratio of induced-acceleration Bond number to the Bond number resulting from the various extraneous disturbances likely to be encountered in any space mission. An optimum solution would demand that the auxiliary thrusters never lose control of the propellant. But for missions requiring long-term coast durations, the continued use of these thrusters could cause excessive weight penalties, and,

thus, their operation may have to be reduced to intermittent durations. During the no-thrust periods, interface disruption and adverse relocation of the propellant due to shutdown transients, orientation maneuvers, atmospheric drag, etc., become definite possibilities. Should interface disruption occur, the auxiliary thrusters would be called upon to reorient or collect the propellant back to the desired location prior to engine restart and venting. A thorough understanding of this reorientation mode by low-level accelerations is of prime importance for successful mission performance.

The subject of reorientation has been discussed in reference 1 and several subsequent papers have presented experimental investigations of the basic liquid-flow patterns prior to liquid impingement at the tank bottom (refs. 2 to 4). These latter investigations assume that the interface has been relocated (by some extraneous disturbance) at the forward or vent portion of the propellant tankage and it has been shown that the initial conditions (i. e., Bond number loading) of the liquid-vapor interface prior to the application of the reorientation acceleration will determine the mode of liquid flow. When the initial interface is relatively flat as indicated by a high Bond number loading, the application of the reorientation acceleration could produce a variety of flow patterns depending on the magnitude of the reorientation Bond number (refs. 2 and 3). Results in this area remain largely qualitative. If the Bond number loading is low, such that the initial liquid-vapor interface is highly curved, quantitative predictions of the reorientation flow can be made (refs. 2 and 4). Further investigations of liquid impingement at the bottom of typical propellant-tank models, however, have indicated that liquid rebounding or geysering could result in circulation of a substantial portion of the liquid rather than quiescent collection (ref. 5). Because of this geysering phenomenon, accurate time estimates of complete propellant reorientation cannot presently be made.

This report presents the results of an experimental investigation of liquid reorientation phenomenon induced by low-gravity environments (i. e., low Bond number) in cylindrical-tank models with concave and convex bottoms. The investigation assumed an initial low Bond number loading with solid-liquid-vapor combinations resulting in contact angles near 0° such that the liquid-vapor interface was highly curved prior to the application of the reorientation acceleration. The results have indicated that, while liquid rebounding or geysering following impingement of the leading edge of the interface at the tank bottom will occur in most practical situations, there exists a distinct region in which geysering will not occur. A criterion consisting essentially of a dimensionless Weber number grouping (i. e., ratio of inertial to capillary forces) successfully delineated the regions of geysering and no geysering within present experimental limitations. Furthermore, quantitative predictions of accumulation rates which would lead to time estimates for complete reorientation depended heavily on the geysering dynamics. Observed qualitative trends in the behavior of the geyser are presented.

SYMBOLS

a	system acceleration, cm/sec^2
a_L	interface leading-edge acceleration, cm/sec^2
Bo	Bond number, $Bo = aR^2/\beta$
D	tank diameter, cm
K, K'	nondimensional constants
L	tank length, cm
R	tank radius, cm
r	geyser radius, cm
t	time, sec
V_c	collected liquid velocity (fig. 2(b)), cm/sec
V_g	geyser tip velocity or growth rate (fig. 2(b)), cm/sec
V_L'	instantaneous leading-edge velocity at impingement or convergence at tank bottom (fig. 2(a)), cm/sec
V_L''	instantaneous leading-edge velocity in convex-bottomed models measured at end of cylindrical portion of tank (fig. 2(a)), cm/sec
V_o	ullage velocity, cm/sec
We	Weber number, $We = (V_L')^2 R/\beta$
X_c	collected liquid depth (fig. 2(b)), cm
X_g	geyser tip displacement (fig. 2(b)), cm
X_L	interface leading-edge displacement from initial 0-g configuration to convergence or impingement, cm
β	specific surface tension, σ/ρ , cm^3/sec^2
ρ	liquid density, g/cm^3
σ	surface tension, dynes/cm

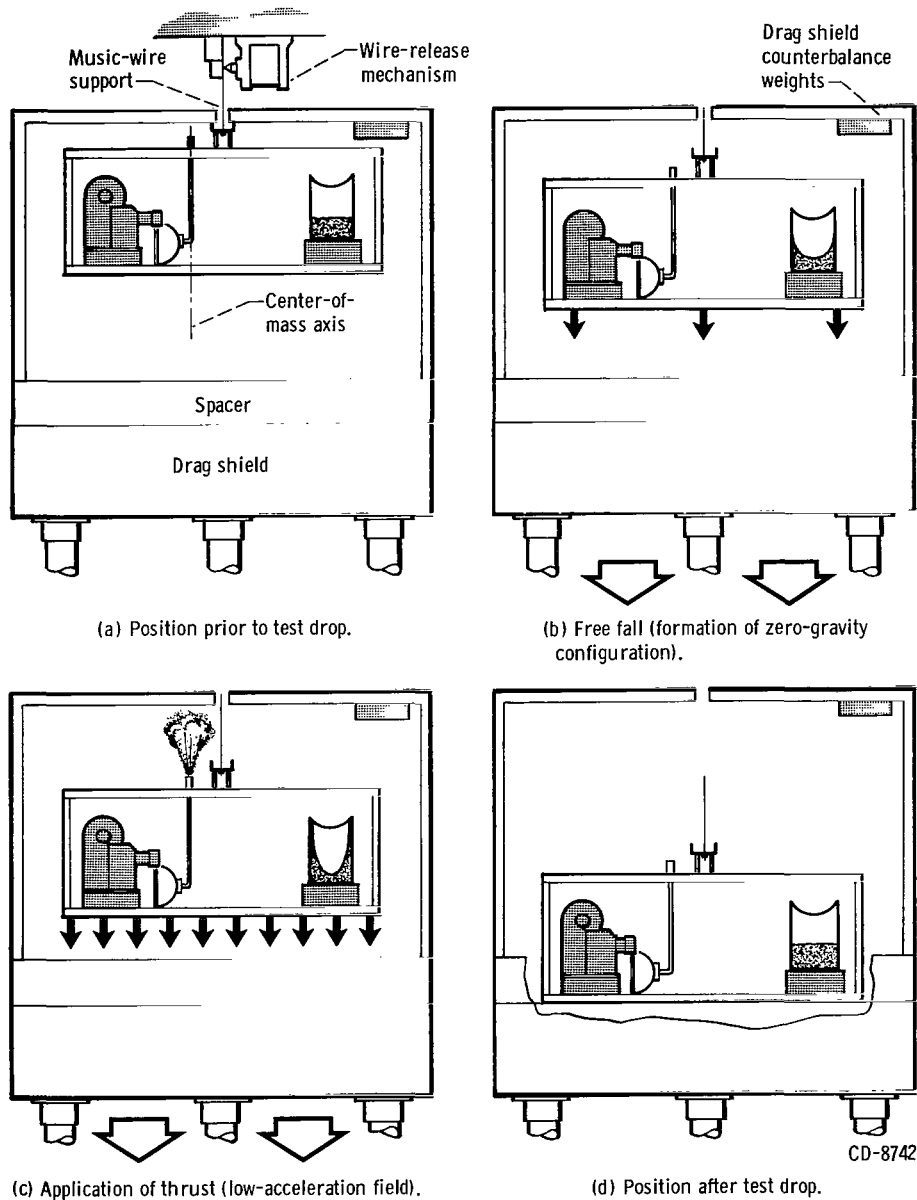


Figure 1. - Schematic drawing showing sequential position of experiment package and drag shield before, during, and after test drop.

APPARATUS AND PROCEDURE

In order to provide the desired initial system conditions (i. e., a highly curved liquid-vapor interface), the investigation was conducted in a 2.3-second zero-gravity drop tower facility (ref. 4). The reorientation acceleration was imposed on the experiment by means of a high-response gaseous-thrust system calibrated on the ground by a combined load-cell, air-bearing stand. The center of mass of the experiment package was located along the thrust axis, and the experiments were carefully aligned so that the imposed acceleration was parallel to the major axis of the test models and was directed normally from the vapor to the liquid phase.

Acceleration as a result of air drag on the experiment package is kept below 10^{-5} g by allowing the package to fall freely inside a protective drag shield, designed with a high weight-to-frontal-area ratio and a low drag coefficient. The drag shield was modified by use of interchangeable spacers to allow for the added relative displacement of the accelerated package. A schematic of the drag shield and experiment package assembly, along with a sequence of events during a test drop, is shown in figure 1.

The magnitude of the reorientation acceleration used in this investigation ranged from approximately 0.01 to 0.1 g and was determined by the 1-g calibration to within 5 percent. This value was substantiated in each test drop by measuring the net accelerated time of the experiment package in the known available distance in the drag shield. Limits to the range of acceleration level were imposed by practical drag-shield spacer additions and reasonable acceleration times in which to observe data. Reorientation Bond numbers in this investigation ranged from approximately 3 to 70.

All data were recorded photographically, and time measurements were obtained by viewing a precision sweep clock with a calibrated accuracy of ± 0.01 second. This method replaces photographic timing marks and eliminates a principal source of error in experiments of this nature. A detailed discussion of operating procedure is given in reference 4.

TABLE I. - PROPERTIES OF TEST LIQUIDS

Liquid	Density at 20° C, ρ , g/cm ³	Surface tension at 20° C, σ , dynes/cm	Specific surface tension, σ/ρ , cm ³ /sec ²
Trichlorotri- fluoroethane	1.58	18.6	11.8
Carbon tetrachloride	1.59	26.8	16.8
Ethanol, anhydrous	.789	22.3	28.3
Methanol	.793	22.6	28.5
Ethanol, 20 percent ^a	.973	39.8	40.9

^aComposition by volume with distilled water.

The liquids and containers employed in this investigation are, in general, representative of the properties and tank geometries of typical liquid-propellant systems. Table I gives the physical properties of the liquids used in this study. All liquids were analytic reagent grade and exhibit static contact angles very near 0° on the containment surfaces. The basic tank models used are shown in

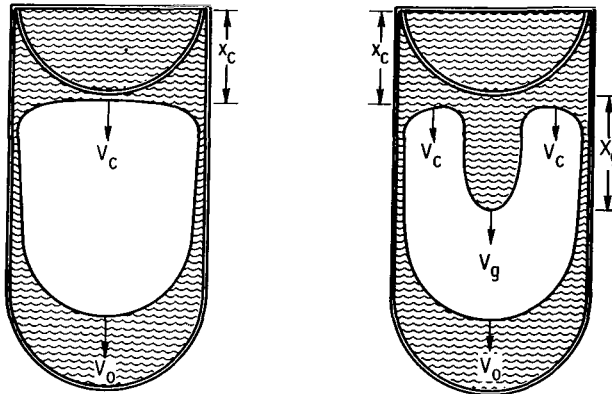
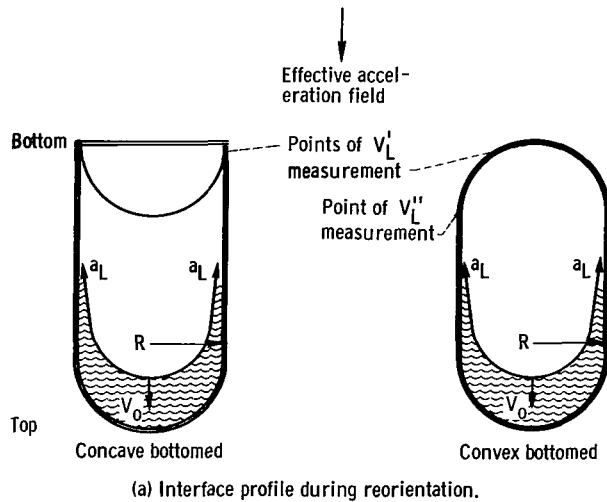


Figure 2. - Basic reorientation profiles.

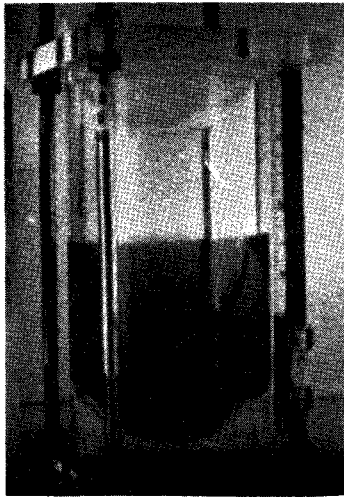
figure 2; data runs with exactly scaled models (e. g. , 1/47 and 1/80 scale models of the Centaur liquid-hydrogen fuel tank) revealed no significant differences in quantitative or qualitative behavior from these hemispherical ended models. The six different model radii employed in this investigation ranged from 1.27 to 5.16 centimeters, and fineness ratios (length-to-diameter ratios) were generally fixed at 2.

RESULTS AND DISCUSSION

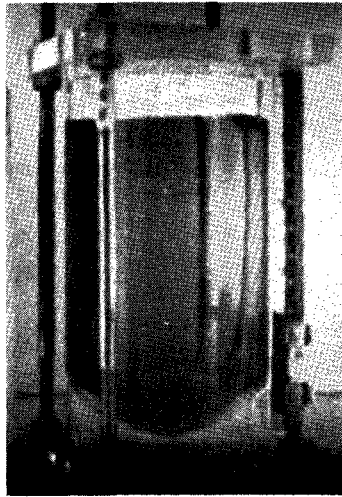
Liquid Reorientation

Liquid rebounding (geysering) and the subsequent recirculation of liquid during reorientation are qualitatively quite ordered and repeatable for the model tank configurations tested. A series of photographs taken from a typical drop tower data run is presented in figure 3 to illustrate the

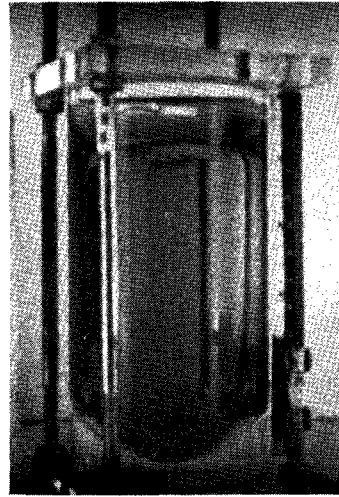
general behavior of the liquid during a reorientation maneuver. Following a short period of weightlessness to allow the interface to approach its zero-gravity configuration (fig. 3(a)), a reorientation acceleration is applied (fig. 3(b)) and causes the liquid to be repositioned. When the leading-edge velocity at impingement at the tank bottom (fig. 3(c)) is sufficiently large, the geyser continues along the center of the tank (fig. 3(f)) and reaches the forward end of the tank or the remaining receding liquid (fig. 3(g)), and liquid recirculation finally results (fig. 3(h)). Geyser tip displacement data for this run are presented in figure 4. The constant geyser velocity obtained in this test indicates that the geyser momentum is dominant and effects of acceleration, surface tension, viscosity, etc., are negligible. In this particular test (Bo , 18; fill ratio, 45 percent liquid;



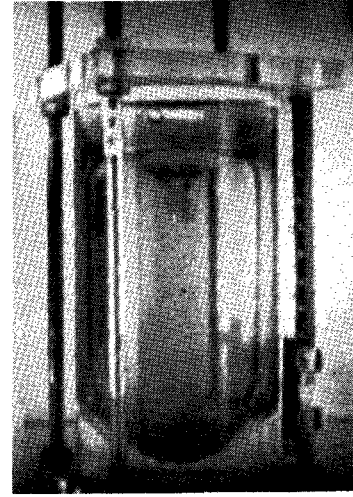
(a) 0-g configuration.



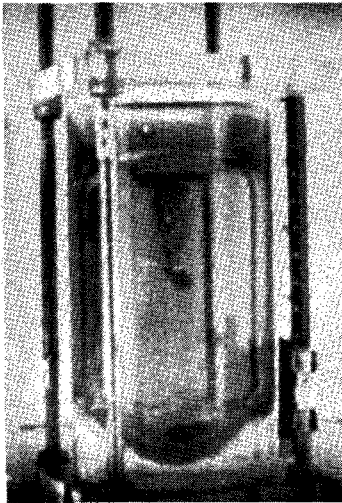
(b) Application of reorientation thrust.



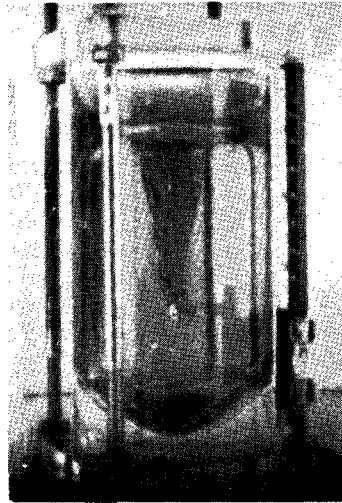
(c) Leading-edge impingement.



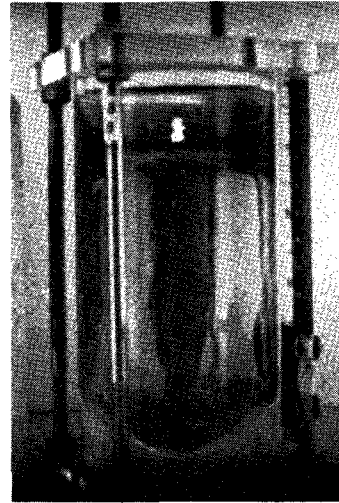
(d) Initiation of geyser.



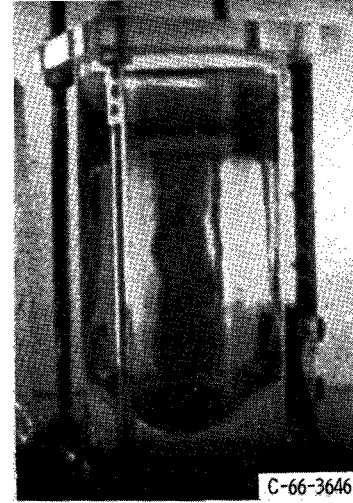
(e) Geyser formation.



(f) Geyser progression.



(g) Geyser impingement.



(h) Recirculation.

C-66-3646

Figure 3. - Reorientation process during representative data test, including formation and recirculation.

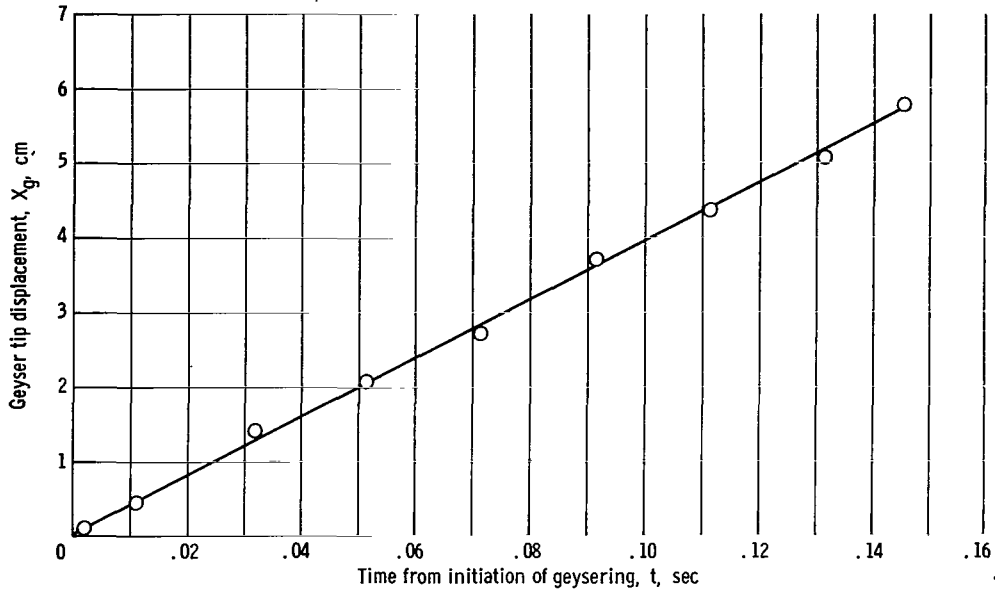


Figure 4. - Geyser-tip displacement characteristics during representative data test.

concave-bottomed model), the data illustrate the inherent quantitative complexity of the reorientation process as well as the obvious dependence of collected liquid on the geyser dynamics. As can be seen from figure 3, while some liquid is being accumulated or collected as desired at the tank bottom, geysering greatly reduces the rate of this collection. In general, the actual reorientation process and, specifically, the actual collection rate depend on the magnitude of the reorientation Bond number, the percent of liquid in the tank, and the tank geometry.

The severity of geysering is directly dependent on V'_L , the magnitude of the instantaneous leading-edge velocity immediately prior to impingement or convergence at the tank bottom (fig. 2). The magnitude of this velocity can be obtained from a knowledge of the volume of residual liquid and by use of the relation (ref. 4)

$$a_L = \frac{3.8 V_o^2}{R} \quad (1)$$

where a_L is the acceleration rate of the leading edge and V_o is the ullage velocity given by

$$V_o = 0.48(aR)^{1/2} \left[1 - \left(\frac{0.84}{Bo} \right)^{Bo/4.7} \right] \quad (2)$$

The time allowed for the interface to approach its 0-g configuration was generally not sufficient to ensure completely quiescent interface conditions. Because of the initial velocity of the interface, V_L' was measured directly, even though it did remain closely approximated by equation (1). In concave-bottomed models, V_L' was obtained graphically from observed leading-edge displacement curves. But in convex-bottomed models, in order to avoid measurement errors in the leading-edge displacement around the hemispherical portion of these models, V_L' was obtained by the relation

$$V_L' = \left[(V_L'')^2 + 2a_L R \right]^{1/2} \quad (3)$$

where V_L'' is the measured velocity at the point shown in figure 2. This relation assumes that the constrained leading-edge motion in the hemispherical portion of the model is similar to that in the cylindrical portion.

While viscosity would undoubtedly be expected to play some role in equations (1) to (3) and in the overall dynamics of reorientation, no significant effect was noted for the liquids used in this study, which have viscosities of the order of 1 centipoise.

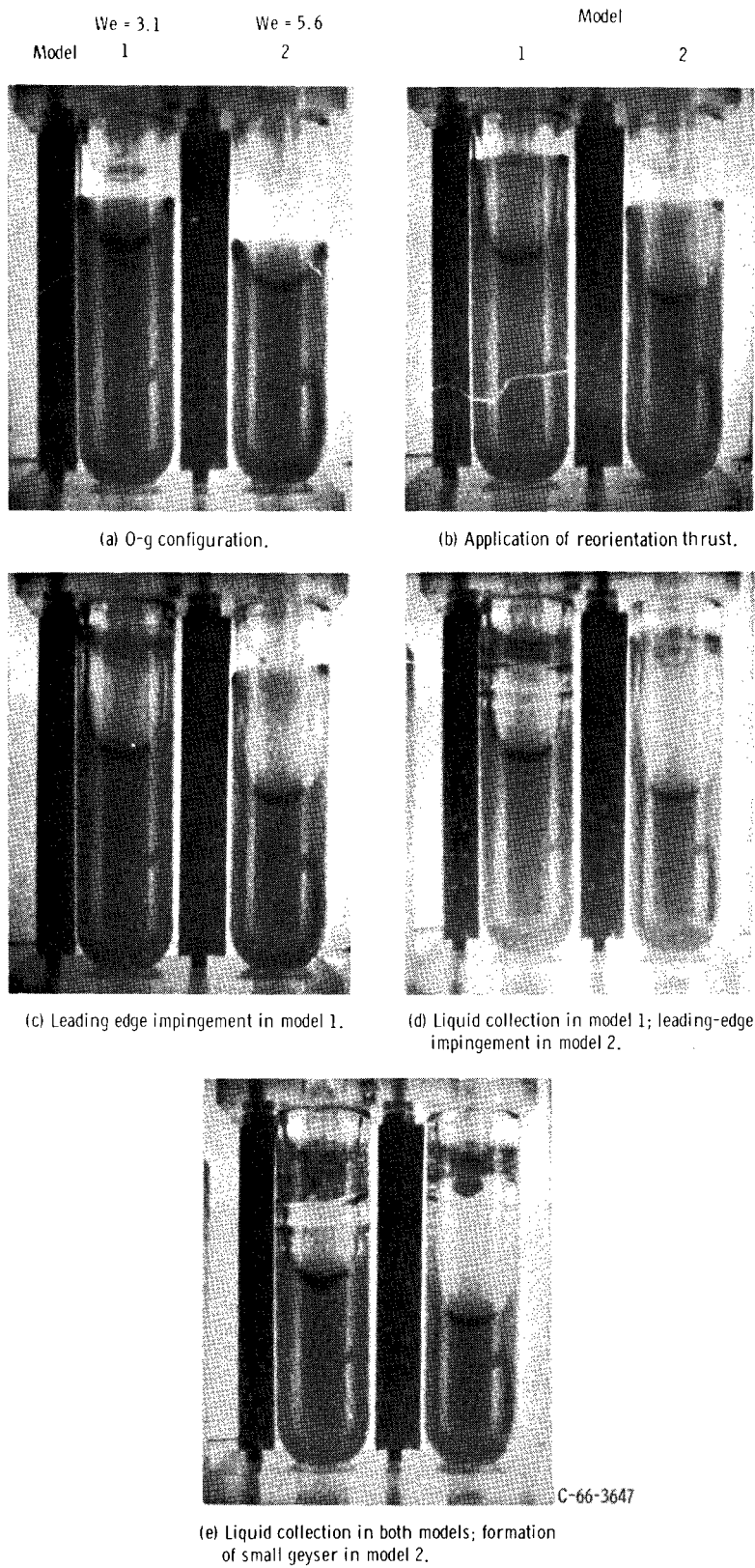
Criterion for Geyser Formation

An investigation of the dependence of geyser formation on the leading-edge liquid velocity V_L' revealed the existence of a critical velocity below which no geyser formed. (The term no geyser is defined in this report, because of practical measurement limitations, as a condition where no geysers are formed of a height greater than $1/4 R$.)

Furthermore, this critical velocity was a function of the specific surface tension of the liquid and the radius of the tank, which indicated that surface tension impedes the formation of geysers subject to the magnitude of the liquid rebounding momentum. A convenient scaling parameter which can be used to describe the relative effects of these variables is the Weber number We , defined in this case as

$$We = \frac{(V_L')^2 R}{\beta} \quad (4)$$

The dimensionless Weber number grouping represents the ratio of inertial-flow forces to surface-tension forces and, in this instance, provides an indication of the relative importance of rebound momentum to the restraining surface tension.



C-66-3647

Figure 5. - Effect of instantaneous leading-edge velocity on geyser formation in concave-bottomed models.

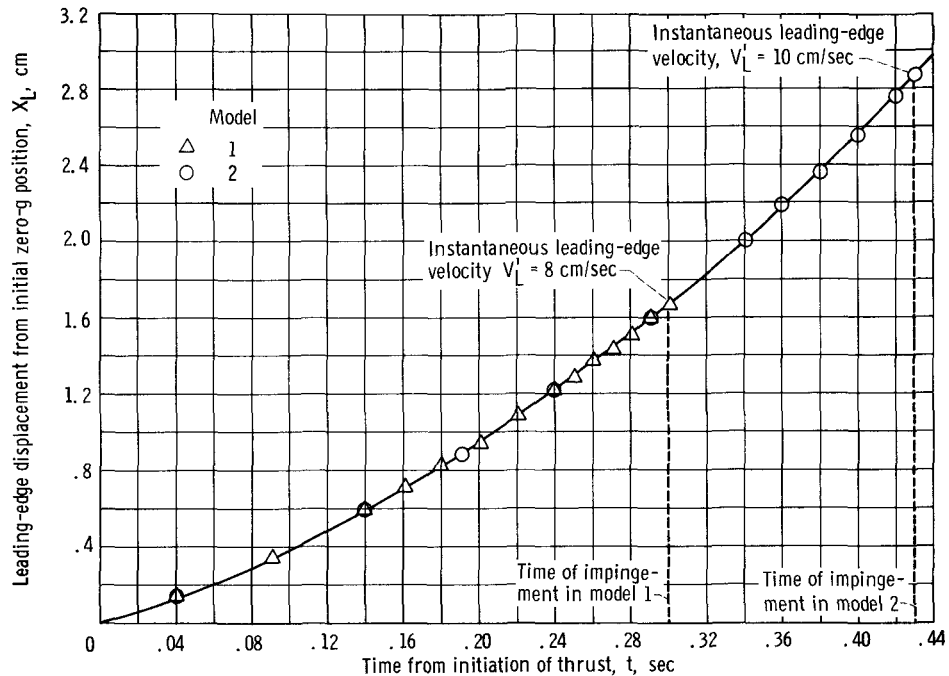


Figure 6. - Leading-edge displacement characteristics during representative data test.



Figure 7. - Effect of instantaneous leading-edge velocity on geyser formation in convex-bottomed models.

Figure 5 illustrates the dependence of geyser formation on the Weber number grouping in concave-bottom models. Both models pictured were subjected to the same reorientation conditions (i. e., the same α , R , and β) so that the acceleration rates of the leading edge in each were equal. The models, however, did contain different initial liquid levels or fillings (fig. 5(a)) that generated different values of V_L' in each model, as can be seen in figure 6. The V_L' observed in model 2 resulted in the formation of a geyser, while the smaller V_L' in model 1 resulted in essentially quiescent collection (fig. 5(e)).

A similar result for convex-bottomed models is shown in figure 7, in which both the absence and the formation of a geyser is exhibited. These models were also subjected to the same reorientation Bond number but contained different initial liquid levels so that different values of V_L' were obtained.

This method of bracketing the critical velocity for particular reorientation conditions was extended over the available range of test liquids and tank sizes, and

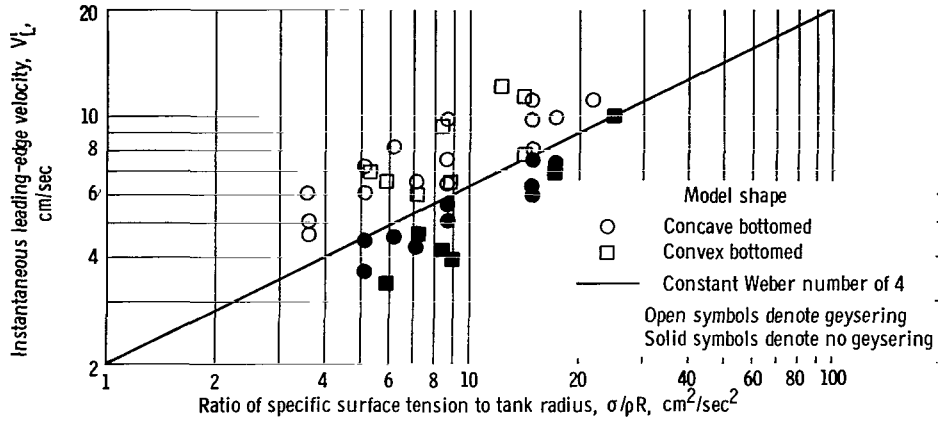


Figure 8. - Geysier formation delineated by Weber number criterion.

the data obtained are presented in figure 8. This figure shows that all the geysers that were formed occurred only when the value of the Weber number for that system was greater than 4, which indicated that above this value surface tension is not large enough to inhibit completely the rebound flow momentum. Conversely, no geysers occurred when the Weber number was less than 4, which indicated that surface tension was dominant at this level. These results establish the Weber number as a criterion that can be used to predict the formation of geysering in the configurations tested.

It should be noted that the available experimental range of V_L' for particular values of β/R was limited both by the range of attainable Bond numbers and by practical liquid-filling levels. The limitations on liquid filling levels were imposed by the necessity of allowing some minimum distance for the leading edge to move during reorientation in order to ensure accuracy in the measurement of V_L' and by the condition that the proximity of the zero-gravity interface to the tank top did not distort its steady-state configuration. The distance values representing maximum and minimum fillings were experimentally determined to be $X_L = 1/3 R$ and $X_L = 5/2 R$, respectively, in model tanks with specified length-to-diameter ratios of 2.

Geysier Flow Regimes

The actual value of the Weber number parameter can further be used to obtain a general classification of the various geysier flow regimes which were experimentally observed. A summary of the results of a series of reorientation experiments at various Weber numbers is presented in figure 9. The general flow patterns represented were in concave-bottomed models with a specified length-to-diameter ratio of 2 and observed over a range of reorientation Bond numbers from 3 to 56.

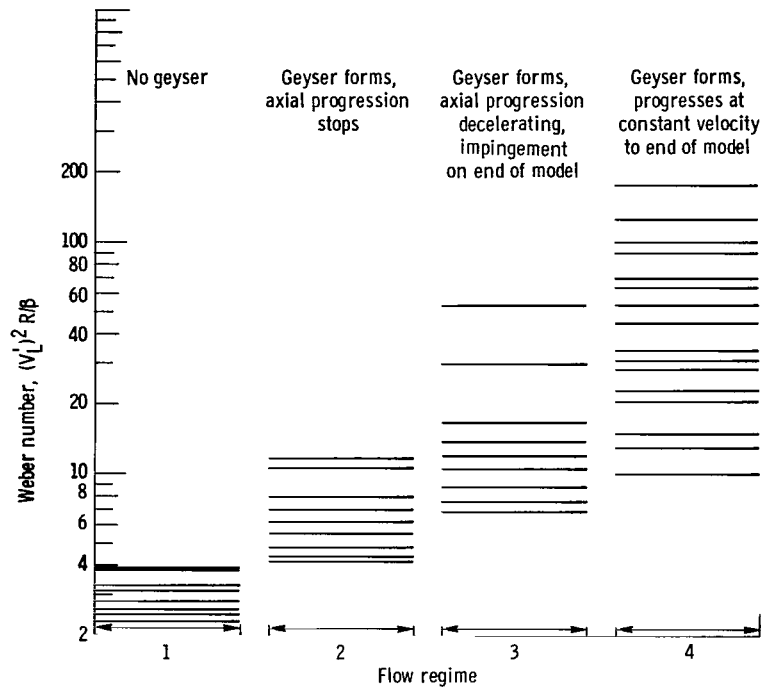


Figure 9. - General classification of observed geyser flow in concave-bottomed models. Length to diameter ratio, 2.

As shown in figure 9, when the Weber number of the system was greater than 4 but less than 7, a geyser always formed and grew to some maximum height above the collected liquid surface, where it remained axially stationary with respect to the tank until finally it either receded or was engulfed by the advancing accumulated liquid (the latter condition is dependent upon the volume of leading-edge liquid available). Whenever the axial progression of the geyser was halted or restricted, the width of the geyser increased proportionally indicating that liquid continued to rebound.

At values of the Weber number greater than 7 the probability of the geyser stopping decreased, although in some instances the geyser tip displacement rate was decelerating before its impingement on the tank forward surface or the receding ullage interface (flow regime 3 in fig. 9). As the system Weber number was further increased, the geyser tip progressed at a constant velocity (fig. 4, p. 8) until impingement, at which time a liquid recirculation pattern was established. This is noted as flow regime 4 in figure 9 and indicates that, for these higher Weber numbers, surface tension is becoming negligible in comparison to geyser momentum.

Concurrent with these observations of geyser behavior were measurements of the geyser tip progression rate (e. g., fig. 4) which, in all cases, was initially linear. The recorded measurements of these velocities are presented in figure 10. From this figure, it is evident that the growth rate of the geyser V_g for specific values of V_L^1 was decreased when the specific surface tension of the liquid was increased and also when the radius of the tank was decreased. For increasing values of V_L^1 , the ratio of V_g to V_L^1

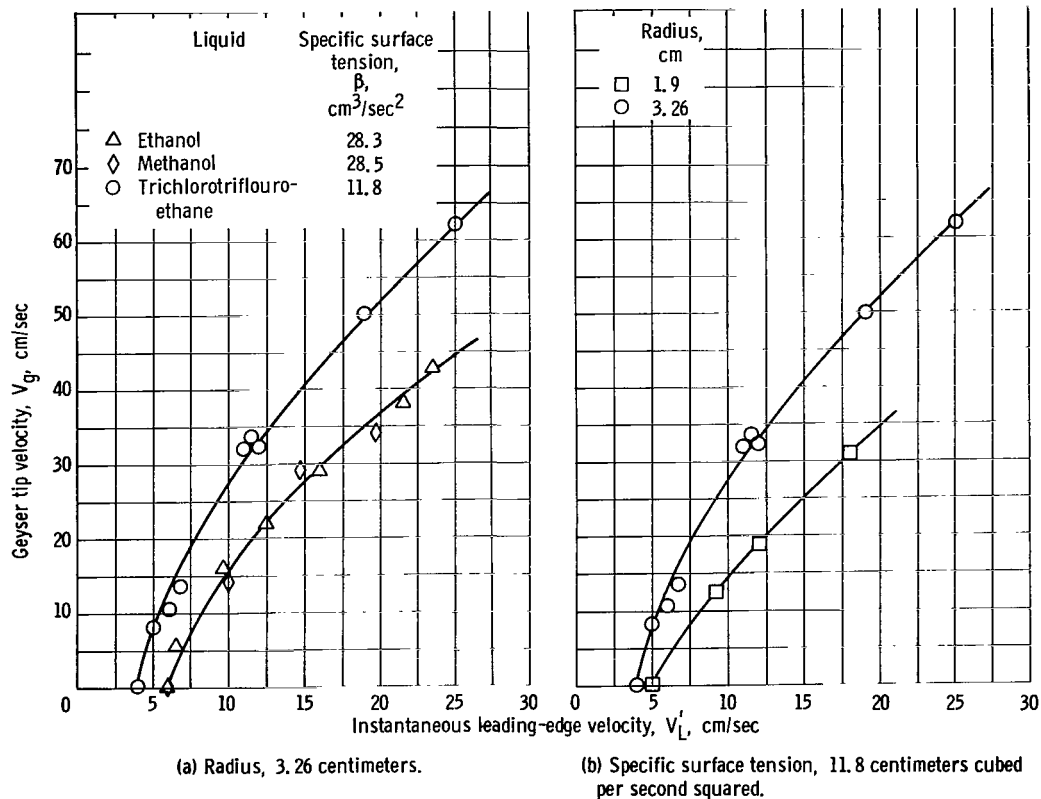


Figure 10. - Effects of liquid properties and tank size on geyser velocity.

appears to be approaching a constant. These trends are presented because they indicate the significance of surface tension in determining the severity or growth rate of geysering and further establish the validity of the Weber number as a criterion for predicting geyser formation and profile.

It is interesting to note that, in the range of viscosities tested, viscous forces had no detectable effects; this fact is evidenced by the similarity in results achieved with both ethanol and methanol (fig. 8), whose viscosities differ by a factor of 2 (i. e., 1.2 and 0.6 cP, respectively).

Collection Rate

It has been observed that all reorientation attempts do result in some accumulation of liquid in the bottom of the tank and that, as long as there exists some reservoir of liquid at the top of the tank, liquid is being collected at a linear rate (V_c in fig. 2(b), p. 6). In those instances where a geyser will occur, as predicted by the Weber number criterion, the estimation of a collection rate is extremely difficult. Any analytical solu-

tion, if at all possible, will depend heavily on experimental observations. Accurate time estimates for complete liquid reorientation, including the decay of the geyser and recirculation flow, are presently not possible because of the lack of sufficient test time in zero gravity to obtain complete information. However, significant experimental data regarding collection rate have been obtained and certain trends have been noted. Estimates of collection rates will depend heavily on the geyser flow regimes given in figure 9.

Low Weber number systems ($We < 4$). - Maximum collection rate efficiency will obviously occur for those reorientation conditions where there is no geyser. In these instances, an ideal collection rate may be predicted if it is assumed that the profile of the interface remains a constant throughout the reorientation mode and that the ullage velocity remains constant independent of tank extremity effects. (This latter assumption is discussed in ref. 2, where corrections for tank extremities are presented.) Under these assumptions, conservation of liquid volume would demand that the collection rate be identical to the ullage velocity, or, by using equation (2),

$$V_c = V_o = 0.48(aR)^{1/2} \left[1 - \left(\frac{0.84}{Bo} \right)^{Bo/4.7} \right] \quad (5)$$

If the reorientation Bond number and percentage of residual liquid are known, an estimate for complete reorientation time can be made by using equation (5) and the appropriate leading-edge displacement times.

Intermediate Weber number systems ($4 < We < 30$). - For those reorientation situations that result in a geyser (i. e., $We > 4$), the estimation of a collection rate becomes extremely difficult as some portion of the collected liquid goes into the geyser. In this defined intermediate Weber number region, the geyser dynamics are highly nonlinear. Based on the observed dynamics of geysering in this region, there exists no simple relation describing the maximum extension of the geyser. The geyser maximum height is apparently proportional to V_L' and inversely proportional to the specific surface tension of the liquid. However, the maximum extension of the geyser is also a function of the unknown accumulated liquid depth and depends further on the ill defined geometry of the geyser. The latter is typically shown in figures 3(e) and (f) (p. 7). The collection rate is directly dependent on the geyser dynamics and, because in this Weber number region the dynamics are not fully understood, no concrete collection rate data can be presented.

High Weber number systems ($We > 30$). - If the Weber number based on V_L' is large, that is, greater than approximately 30, the geyser will generally progress at a constant velocity (in tanks with $L/D = 2$). If the ullage velocity is assumed constant and if the leading-edge flow is not distorted throughout the reorientation process, then con-

servation of volume flow yields the approximation

$$V_o \pi R^2 = V_g \pi r^2 + V_c \pi R^2 \quad (6)$$

where r is the radius of the geyser column and V_c is measured in the pure cylindrical portion of the tankage. The geyser radius is both time and surface tension dependent with no simple relation apparent. Data runs have consistently shown, however, that the average geyser radius is between $1/4 R$ and $1/2 R$ and may effectively be regarded as constant during a particular reorientation process after recirculation has been established. Furthermore, the geyser velocity was related to the velocity of the leading edge at impingement V_L' by

$$V_g = K' V_L' \quad (7)$$

where K' ranges from 1.9 to 2.9. Again, as evidenced by figure 10, K' is some function of liquid properties and tank geometry. The average value of K' obtained was approximately 2.5. These empirical ratios for V_g/V_L' and r/R lead to a convenient defining parameter:

$$K = \frac{V_g r^2}{V_L' R^2} \quad (8)$$

such that equation (6) may be rewritten

$$V_c \pi R^2 = V_o \pi R^2 - K V_L' \pi R^2 \quad (9)$$

or

$$V_c = V_o - K V_L' \quad (10)$$

Ideally,

$$V_L' = (2a_L X_L)^{1/2} \quad (11)$$

where X_L is the leading-edge displacement between its initial 0-g position and the point

of impingement or convergence at the tank bottom. Substituting for a_L from equation (1) yields

$$V_L' = 2.76 V_o \left(\frac{X_L}{R} \right)^{1/2} \quad (12)$$

and, therefore,

$$V_c = V_o \left[1 - 2.76 K \left(\frac{X_L}{R} \right)^{1/2} \right] \quad We > 30 \quad (13)$$

Actual values of K obtained from measured values of V_c , V_o , and V_L' in concave-bottomed models by using equation (10) varied from 0.15 to 0.35 and generally decreased with increasing Weber number. If the reorientation Bond number and percentage of residual liquid are known, approximate estimates of the amount of liquid collected after a given time can be made by using equation (13) (under the stated assumptions) and the initial leading-edge displacement time. Complete reorientation time, however, remains undefined as the decay characteristics of the recirculation mode are not presently known.

Comparison of collection Bond numbers. - For the situation in which the collection Weber number is less than 4 or greater than 30, equations (5) and (13) may be used within the observed limitations to calculate initial collection rates. For a given set of conditions (tank size, filling, etc.) these equations permit a comparison of the collection time and the required collection impulse for a high and low Bond number collection. The results of calculations of the time and impulse required to collect an initial quantity of liquid for both a high and a low Bond number case are presented in figure 11. For the purpose of this example, a hemispherically concave-bottomed tank 10 feet (304.8 cm) in diameter was used which contained a typical wetting-liquid propellant ($\beta = 33 \text{ cm}^3/\text{sec}^2$) positioned at its vent end. A liquid-fill ratio was assumed such that the leading edge of the zero-gravity liquid-vapor interface was initially one radius from the tank bottom (i. e., $X_L = R$). To facilitate the calculation of a collection rate, the values of the comparative Bond numbers were chosen to be 4 and 100 (i. e., acceleration levels of 6×10^{-6} and $1.5 \times 10^{-4} \text{ g}$, respectively) so that the predicted geyser flows in each case were within the regimes of no geysering ($We = 3.87$) and constant-velocity geysering ($We = 176$), respectively.

It can be seen from figure 11 that, while the time required to collect the initial quantity of liquid (i. e., $R^2(R + 30 \text{ cm})$) was considerably less for the higher Bond number case, the impulse to mass ratio required to achieve this objective with the higher Bond number was much greater. The relative importance of collection time and collection impulse depends on the mission requirements and the propellants involved. For those missions

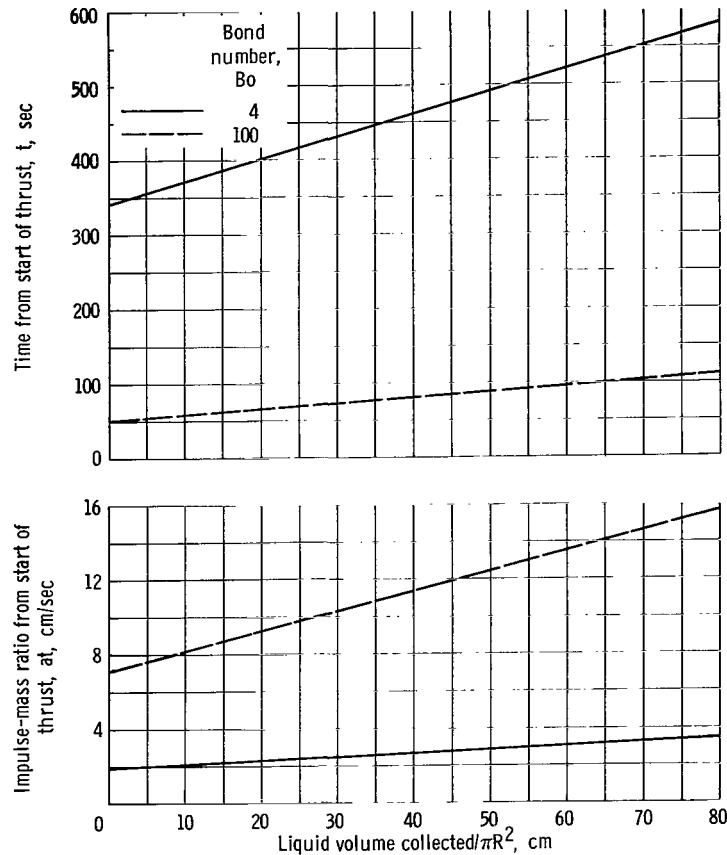


Figure 11. - Time and total impulse required to collect liquid as function of collection Bond number.

that require multiple restarts and use storable propellants which require no venting, it would appear that the total impulse for collection would be important and that engine starting times could be predicted sufficiently in advance that low Bond number collection could be used. Even in the case of cryogenics venting times could be predicted from pressure rise rates so that the more orderly collection obtained at low Bond numbers could be used. For this condition the collection process is sufficiently linear that equation (5) permits reasonable estimates of total collection time.

Quite obviously, an idealized situation has been presented. It should be evident that the choice of a collection Bond number will depend heavily on specific mission requirements and restrictions.

Depletion of leading-edge flow. - It has tacitly been assumed in the preceding discussions that there exists sufficient residual liquid in the top of the tank that the leading-edge flow is continuous. If the leading-edge flow is depleted either because the residual liquid supply is relatively small or, in the case of large system Weber numbers, because the geyser has not been recirculated (or a combination of these factors), the collection rate as expected goes to zero. Calculations of the ullage velocity (eq. (2)), the instan-

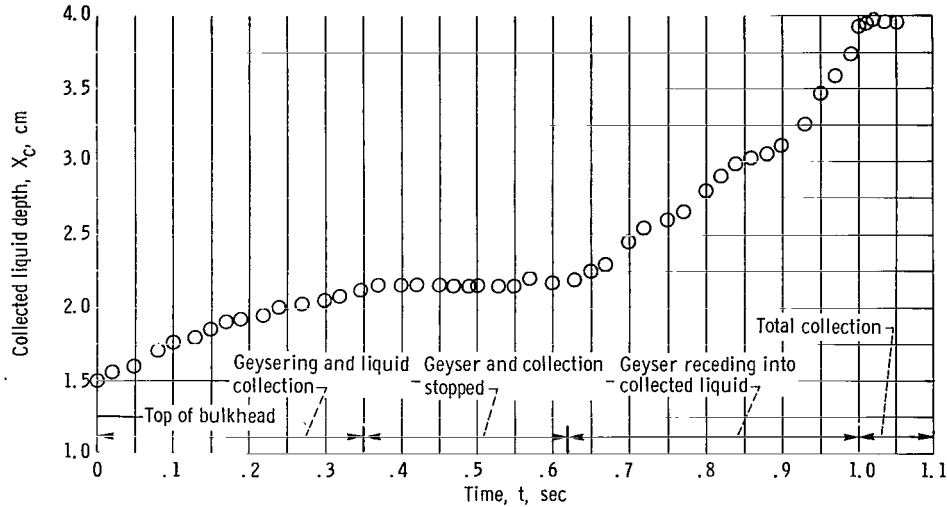


Figure 12. - Effects of geyser dynamics on liquid collection rate.

taneous leading-edge velocity (eq. (12)), and the geyser velocity (given by the approximation in eq. (7)) provide a relative indication of whether this situation will occur. A specific instance illustrating the effect of leading-edge depletion is shown in figure 12; the actual system Weber number is 29 and, while the geyser does reach the tank top, it is decelerating significantly, which indicates that it is rapidly approaching its maximum height. Depletion of the leading-edge flow (in this instance, the ullage has reached the top of the tank) results in an essentially zero collection rate, followed after some time by a substantial rise caused by the decay of the geyser.

SUMMARY OF RESULTS

An experimental investigation was conducted of the mechanism of liquid reorientation from an initially highly curved interface by low-level accelerations. The study was conducted by using several geometrical propellant-tank models, with radii ranging from 1.27 to 5.16 centimeters, and liquids possessing near 0° contact angles on the tank materials and having viscosities of the order of unity. The following results were obtained:

1. Liquid rebounding or geysering can occur during liquid reorientation by the application of low-level accelerations.
2. A criterion consisting essentially of a dimensionless Weber number grouping based on liquid flow conditions at the tank bottom delineated the regions of geysering and no geysering.
3. The value of the Weber number which delineates the regions of geysering and no geysering was empirically determined to be 4 in both concave- and convex-bottomed models.

4. Quantitative results of liquid accumulation rates which would allow time estimates for complete liquid reorientation were heavily dependent on overall geyser dynamics.

Lewis Research Center,
National Aeronautics and Space Administration,
Cleveland, Ohio, September 16, 1966,
124-09-03-01-22.

REFERENCES

1. Gluck, D. F.; and Gille, J. P.: Fluid Mechanics of Zero G Propellant Transfer in Spacecraft Propulsion Systems. Paper No. 862A, SAE, Apr. 1964.
2. Hollister, M. P.; and Satterlee, H. M.: Low-Gravity Liquid Reorientation. Paper presented at USAF/OSR and Lockheed Missiles and Space Company Symposium on Fluid Mechanics and Heat Transfer Under Low Gravitational Conditions, Palo Alto, Calif., June 24-25, 1965.
3. Bowman, T. E.: Liquid Settling in Large Tanks. Paper presented at USAF/OSR and Lockheed Missiles and Space Company Symposium on Fluid Mechanics and Heat Transfer Under Low Gravitational Conditions, Palo Alto, Calif., June 24-25, 1965.
4. Masica, William J.; and Petrash, Donald A.: Motion of Liquid-Vapor Interface in Response to Imposed Acceleration. NASA TN D-3005, 1965.
5. Masica, William J.; and Salzman, Jack A.: An Experimental Investigation of the Dynamic Behavior of the Liquid-Vapor Interface Under Adverse Low-Gravitational Conditions. Paper presented at USAF/OSR and Lockheed Missiles and Space Company Symposium on Fluid Mechanics and Heat Transfer Under Low Gravitational Conditions, Palo Alto, Calif., June 24-25, 1965.

"The aeronautical and space activities of the United States shall be conducted so as to contribute . . . to the expansion of human knowledge of phenomena in the atmosphere and space. The Administration shall provide for the widest practicable and appropriate dissemination of information concerning its activities and the results thereof."

—NATIONAL AERONAUTICS AND SPACE ACT OF 1958

NASA SCIENTIFIC AND TECHNICAL PUBLICATIONS

TECHNICAL REPORTS: Scientific and technical information considered important, complete, and a lasting contribution to existing knowledge.

TECHNICAL NOTES: Information less broad in scope but nevertheless of importance as a contribution to existing knowledge.

TECHNICAL MEMORANDUMS: Information receiving limited distribution because of preliminary data, security classification, or other reasons.

CONTRACTOR REPORTS: Technical information generated in connection with a NASA contract or grant and released under NASA auspices.

TECHNICAL TRANSLATIONS: Information published in a foreign language considered to merit NASA distribution in English.

TECHNICAL REPRINTS: Information derived from NASA activities and initially published in the form of journal articles.

SPECIAL PUBLICATIONS: Information derived from or of value to NASA activities but not necessarily reporting the results of individual NASA-programmed scientific efforts. Publications include conference proceedings, monographs, data compilations, handbooks, sourcebooks, and special bibliographies.

Details on the availability of these publications may be obtained from:

SCIENTIFIC AND TECHNICAL INFORMATION DIVISION
NATIONAL AERONAUTICS AND SPACE ADMINISTRATION
Washington, D.C. 20546